UNIVERSITY OF MEDICINE AND PHARMACY
"CAROL DAVILA", BUCHAREST
DOCTORAL SCHOOL FIELD OF PHARMACY

PHD THESIS SUMMARY

INTERDISCIPLINARY STUDIES ON SOME TETRAPYROLIC COMPOUNDS WITH POTENTIAL APPLICABILITY IN ONCOLOGICAL DERMATOLOGY

PhD supervisor:
PROF. DR. DUMITRU LUPULIASA

PhD student:
ANDREEA MIHAELA BURLOIU (POHRIB)

2024

CONTENTS OF THE DOCTORAL THESIS

INTRODUCTION

Recent statistics highlight cancer as the leading cause of death worldwide. Of the 20 million new cancer cases identified in 2022, approximately 10 million cancer deaths were recorded. Global cancer burden is expected to be 28.4 million cases in 2040, with a 42% increase from 2022 (Bray et al., 2024; Kim and Chang, 2023). Therefore, the efforts of specialists to develop innovative strategies for the dissemination of cancer prevention methods and providing new antitumor compounds, are essential in the efficient management of this pathology.

Non-melanoma skin cancers are classified by world statistics among the most common forms of cancer with an evolution of one million new cases annually reported. (Bray et al., 2024). This type of cancers includes basal cell carcinoma, cutaneous squamous cell carcinoma, actinic keratoses, cutaneous lymphomas, Kaposi's sarcoma and angiosarcoma (Esteva et al., 2017; Zink, 2019).

The variability of the components involved in the appearance of skin tumors makes it difficult to identify their triggering factor and requires dermato-oncology specialists to develop new therapeutic strategies as alternatives to classic therapies.

Photodynamic therapy with similar structures protoporphyrin IX, is a promising alternative to conventional antitumor approaches, due to long-term therapeutic efficiency and minimal toxic effects in relation to healthy cells. Topical application of PSs offers the advantage of field PDT and decreases the risk of systemic phototoxicity. Topical PDT using aminolevulinic acid (ALA) or its methyl ester proved to be a frequent option for actinic keratosis and non-melanoma skin cancer treatment, but the clinical potential of ALA is limited by the low rate of its uptake in cells and its poor bioavailability, both attributed to its structural characteristics and hydrophilic nature (Luo et al., 2024).

A series of pharmaceutical products containing tetrapyrrole-based photosensitizers (Purlytin®, Foscan®, Foslip®) are currently used in topical photodynamic therapy. Tetrapyrrole structures have good selectivity for tumor cells, low cytotoxicity in the dark, excellent photophysical properties with a high molar absorption coefficient in the phototherapeutic window (600–800 nm), and good efficiency in promoting reactive oxygen species (Sarbadhikary et al., 2021).

Despite these advantages, the application of porphyrin derivatives in topical PDT has been limited because of their reduced solubility in biological media and molecular aggregation tendency with a negative effect on uptake in tumor cells (Kim et al., 2023). Due to the poor penetration of photosensitizer into the cutaneous tissues, the therapeutic effectiveness of topical PDT will be limited only to superficial skin lesions. These disadvantages can be limited by implementing drug-design strategies to obtain new molecules, with structural architectures associated with a hydrophilic/lipophilic ratio favorable to efficient cellular internalization (Yano et al., 2011).

As an alternative to structural changes, the use of pharmaceutical nanotechnologies could be an optimal approach to ensure a good release of the PS molecule in the tumor tissues. Polymeric nanocarriers have the ability to enhance the solubility of the porphyrinic photosensitizer, offer greater capacity for hydrophobic dissolution, enhance bioavailability, and ensure controlled release in the tumoral tissues. Hydrophilic molecules like polyethylene glycol and polysaccharides are frequently used to enhance the solubility of porphyrin derivatives in biological media (Yang et al., 2023).

Justified by the presented aspects, the main objective of the PhD thesis was the structural, spectral, biological evaluation and formulation of new compounds with applicability in optimized photodynamic therapy of premalignant and malignant skin disorders.

The stages of the studies include:

- the analysis of bibliographic data on the current state of research regarding the identification and therapy of premalignant and malignant skin disorders
- obtaining and *in vitro* evaluation of a new compound with applicability in oncological dermatology
- the selection of tetrapyrrole molecules with applicability in the therapy of premalignant and malignant skin disorders; the study included *in vitro* evaluation of the porphyrins by testing on normal human dermal fibroblasts, normal human keratinocytes, tumor cell lines.
- the formulation of selected porphyrins for topical PDT applications; pharmacotechnical and physico-chemical evaluation of the obtained pharmaceutical forms.
- preliminary *in vitro* release study of porphyrin from HPMC polymer matrix.

The interdisciplinary studies included in the experimental part of the doctoral thesis were carried out in the research laboratories of the Pharmaceutical Technology and Biopharmacy Department, Faculty of Pharmacy, “Victor Babes” National Institute of Pathology and “Ilie Murgulescu” Institute of Physical Chemistry, Romanian Academy; the research was supported by the Romanian Ministry of Research, Innovation and Digitalization through the grant „*Customized photodynamic protocol with innovative porphyrins and redox modulators in premalignant cutaneous disorders - preclinical demonstration*”.

EXPERIMENTAL PART

Chapter 3. Study on obtaining and *in vitro* evaluation of a new compound with applicability in oncological dermatology

In recent years, the development of new photosensitizers with tetrapyrrolic structures has created a multitude of therapeutic perspectives, especially in cancer theranostics (Plekhova et al., 2022). Their structural design, photophysical profile, and strong absorption capacity in the therapeutic window, correlated with their ability to generate reactive oxygen species (ROS) in the presence of molecular oxygen and light, are the main factors behind their therapeutic potential (Sarbadhikary et al., 2021).

Considering the importance of developing new photosensitizers with suitable properties for PDT in non-malignant and malignant skin disorders, in a first stage of doctoral studies, synthesis, *in silico* and *in vitro* evaluation for 5-(2-hydroxy-3-methoxyphenyl)-10,15,20-*tris*-(4-carboxymethylphenyl) porphyrin (P5.2), was performed (Burloiu et al., 2022; Burloiu et al., 2024b).

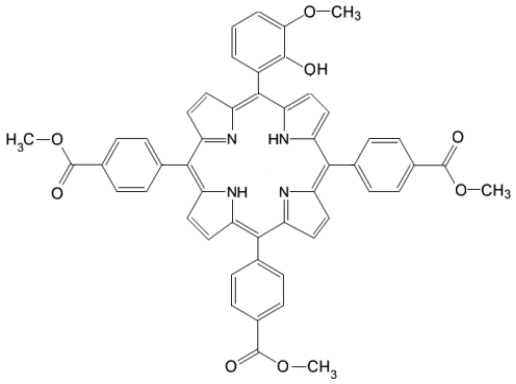

Figure 3.1. The molecular structure of the 5-(2-hydroxy-3-methoxyphenyl)-10,15,20-*tris*-(4-carboxymethylphenyl) porphyrin (P5.2).

Preliminary in silico assessment of the localization potential and antitumor, pharmacokinetic and toxicological profile for a novel porphyrin core compound.

The ability of the porphyrin compound P5.2 to cross the cell membrane was predicted using the PerMM (Permeability of Molecules across Membranes) web server, by simulating the translocation of the P5.2 structure through the lipid bilayer consisting of dioleoyl phosphatidylcholine (Lomize et al., 2019). The used software allowed the calculation of the binding energy of P5.2 to the cell membrane (ΔG, kcal/mol) structure, the permeability coefficient (logPerm), and the generation of the transfer energy (ΔG_{transf}) profile as a function of the distance from the center of the membrane. The simulation results indicated a predicted value of the cell membrane binding energy (ΔG=−6.06 kcal/mol) and permeability coefficient (logPerm=−2.7), suggesting relatively good membrane permeability (Burloiu et al., 2024b). A preliminary computational evaluation of the ADMET profile (absorption, distribution, metabolism, elimination, toxicity) was performed, estimating several pharmacokinetic and

toxicological parameters for the porphyrin derivative P5.2. Topical as well as systemic administration of the compound P5.2 were considered. The models used indicated a good potential for diffusion through the skin, which is relevant in the context of managing premalignant or malignant skin lesions through PDT. After diffusion through the cell membrane, the compound showed the potential for localization at the mitochondrion, thus being able to exert its cytotoxic effect by producing mitochondrial dysfunctions. The investigated porphyrin derivative has a very low probability of producing cutaneous toxicity after topical administration, this aspect is relevant for the applicability of the porphyrin compound, namely the PDT of premalignant and malignant skin disorders. The used models indicated for P5.2 lack of marked toxicity on non-malignant cells after local administration. Molecular docking and molecular dynamics simulations supported the potential antitumor activity of P5.2, which could target the hypoxia-induced tumor-associated carbonic anhydrase IX (Burloiu et al., 2024b).

Obtaining, structural and spectral evaluation of the 5-(2-hydroxy-3-methoxyphenyl)-10,15,20-tris-(4-carboxymethylphenyl) porphyrin.

The technical procedure applied to obtain the porphyrin was initiated by the condensation reaction of pyrrole with 2-hydroxy-3-methoxy-benzaldehyde and methyl 4-formyl benzoate, in a 4:1:3 molar ratio, under microwave irradiation, in an anhydrous environment (Burloiu et al., 2022). The reaction product was dissolved in dichloromethane/ethyl ether mixture (30v/1v), the solution was filtered at normal pressure and the filtrate was concentrated by simple distillation. The separation of the P5.2 from the crude product was achieved by chromatography (Burloiu et al., 2022). P5.2 was obtained with 38% yield and is described by the following spectral characteristics: ^{1}H-NMR, δ_H(400 MHz, $CDCl_3$), ppm: -2.75 (s, 2H), 4.13 (s, 3H), 4.18 (s, 9H), 5,83 (s, 1H), 7.28 (d, 1H), 7.32 (d, 1H), 7.65 (t, 1H), 8.32 (d, 6H), 8.47 (d, 6H), 8.81 (d, 6H); 8.91 (d, H); IR (cm^{-1}): 3424, 3316, 2924, 2853, 1722, 1606, 1558, 1468, 1434, 1402, 1276, 1179, 1100, 1020, 963, 867, 801, 760, 735. UV-Vis $_{(solvent\ PEG200)}$ λ_{max}(nm): 402, 495, 528, 570, 630.

Spectral analysis confirmed the structure of P5.2 and revealed absorption and fluorescence properties suitable for a photosensitizer. Thus, the molecular absorption spectrum of P5.2 (Figure 3.2a) exhibit the typical spectral features of free-base porphyrins, with an intense Soret band at 402 nm, accompanied by other four Q bands in the 496–630 nm spectral region. The presence of a Q band at 630 nm in the UV-Vis spectrum of P5.2 (Figure 3.2a) confirms its absorption potential in the phototherapeutic field, a spectral range of interest for PDT applications. The assessment of the fluorescent properties of P5.2 confirmed the presence of an emission maximum at λ=657nm (Figure 3.2b), a relevant value for a photosensitizer with PDT application.

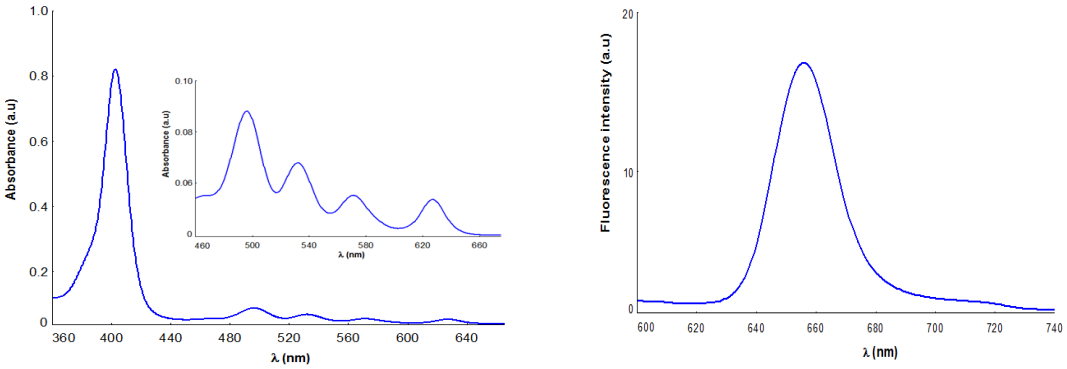

(a) **(b)**

Figure 3.2. (**a**) Absorption spectrum and (**b**) Fluorescence spectrum of P5.2 dissolved in PEG 200, c = 10 µM (λex = 410 nm).

In vitro evaluation of the compound 5-(2-hydroxy-3-methoxyphenyl)-10,15,20-tris-(4-carboxymethylphenyl) porphyrin on cell lines relevant to onco-dermatology

The *in vitro* biological study aimed to evaluate the biocompatibility of the P5.2, its cellular internalization capacity, the potential of a fluorescent cell marker and the cellular effects of photodynamic therapy (PDT) performed with the porphyrin derivative.

The following types of skin-specific adherent cells were used for the *in vitro* experiments: the human skin cell lines HaCaT keratinocytes, Hs27 fibroblasts and B16F10 mouse melanoma tumor cells were used. The experimental methodology applied in the *in vitro* studies is detailed in the reference Burloiu et al. 2024b.

Considering the fluorescent properties of the porphyrinic compound, its incorporation into skin-specific cells was evaluated by flow cytometry.

The experimental results presented in Figure 3.3 confirm the incorporation of the tested porphyrin in all cell types (HaCaT, HS27 and B16F10).

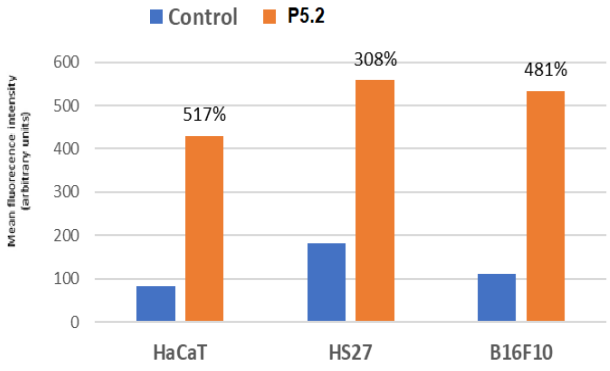

Figure 3.3. Uptake of P5.2 (10 µM) by HaCaT, Hs27 and B16F10 cells. The percentage of the mean fluorescence intensity in P5.2-treated cells relative to the control is provided.

An increase in cellular fluorescence of 517% in HaCaT keratinocytes, of 308% in Hs27 fibroblasts and 481% in B16F10 was observed. The results confirm the potential utility of the porphyrin derivative as a fluorescent marker in normal or malignant skin

cells. Moreover, the cellular uptake of the porphyrin derivative is also an essential condition for its potential use as a PS in PDT.

P5.2 biocompatibility was evaluated by the MTS [(3-(4,5-dimethylthiazol-2-yl)-5-(3- carboxymethoxyphenyl)-2-(4-sulfophenyl)-2H-tetrazolium)] reduction test, which provides information on the number of metabolically active cells in culture, complemented with the lactate dehydrogenase (LDH) release assay, which offers information about the alteration of the plasma membrane integrity in relation to necrotic cell death. The results showed that for concentrations of 10 µM porphyrin, there is no statistically significant change in the release of LDH by any of the investigated cell lines, normal or tumor (Figure 3.4).

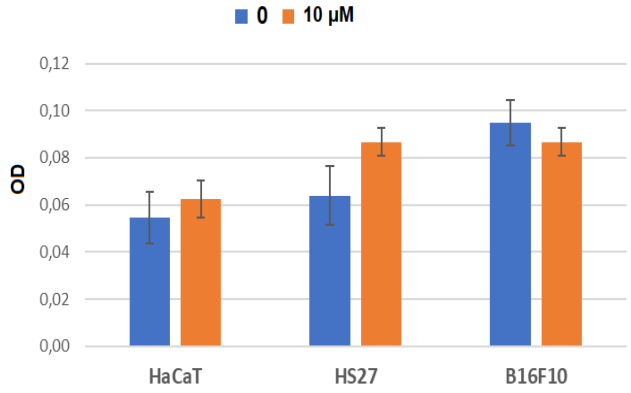

Figure 3.4. LDH release by HaCaT, Hs27 and B16F10 cells treated for 24 h with 10 µM P5.2. The results are presented as mean OD value ± SEM for triplicate samples.

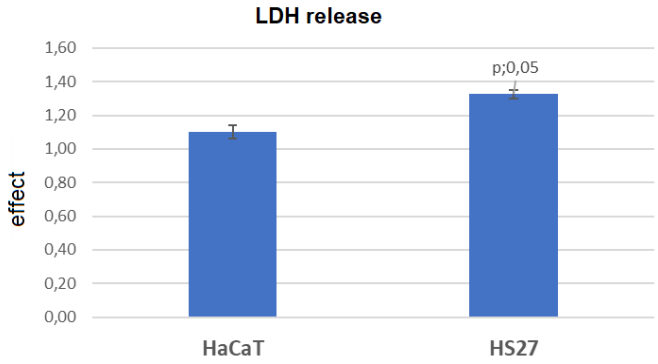

Figure 3.5. Effect of P52 treatment of HaCaT, HS27 cells (c=10 µM, 24h). The results are presented as mean value ± SEM. Differences between cells were considered statistically significant for values of $p<0.05$.

P5.2 is not cytotoxic in "dark" conditions. However, there is a more pronounced tendency to release LDH in the case of Hs27 cells compared to HaCaT cells (Figure 3.5). The effect exerted in vitro by P5.2 on the number of active metabolic cells was also evaluated as a measure of its potential anti-proliferative effects. MTS reduction data showed nominally lower MTS reductions by normal human keratinocytes ($p < 0.05$), while human dermal fibroblasts were not affected at the level of this parameter (Figura

3.6). According to the obtained results, P5.2 can inhibit the proliferation of keratinocytes, thus proving, in addition to fluorescent properties, moderate antiproliferative activity. These properties of the P5.2 have relevance in the case of actinic keratosis characterized by aberrant proliferation of keratinocytes in the epidermis (Dodds et al., 2014).

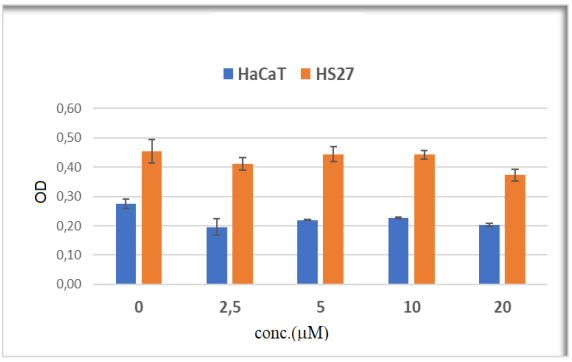

Figure 3.6. MTS reduction by HaCaT and HS27 cells treated for 24h with P5.2 (c=2.5-20µM). Results are presented as mean as mean OD value ± SEM for triplicate samples.

Photodynamic therapy (PDT) was applied to cell cultures using the Modulight ML6600 equipment (Modulight Inc, Tampere, Finland), equipped with a 635 nm laser, controlled in terms of fluence (10 J/cm^2) and irradiance (50 mW/cm^2) (Dobre, et al., 2021). MTS reduction data showed a decrease to 72% of the number of metabolically active cells at 24 h after PDT, accompanied by an approximately 3-fold increase in LDH release (Figure 3.7).

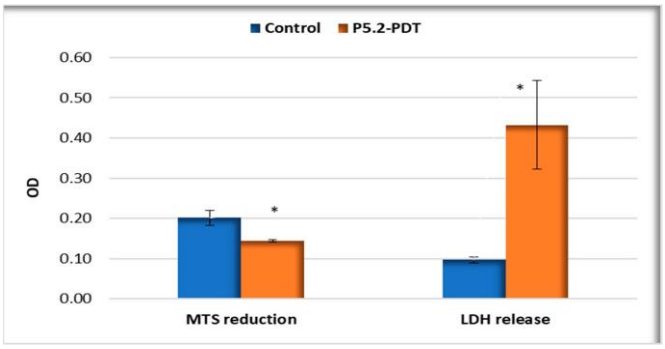

Figure 3.7. MTS reduction and LDH release by HaCaT keratinocytes loaded with P5.2 (10 µM), subjected to PDT (10 J/cm^2, 50 mW/cm^2) and further analyzed at 24 h after treatment. The results are presented as mean OD value ± SEM for triplicate samples. * $p < 0.05$ (Student *t*-test).

Therefore, experimental data highlight the potential of P5.2 to induce a moderate photosensitization of normal keratinocytes. The *in vitro* assessment on cells relevant for premalignant and malignant skin conditions, revealed a good cellular internalization and a good biocompatibility for the tested compound. The good fluorescent profile and cellular incorporation capacity recommend P5.2 as a fluorescent marker in premalignant and malignant skin conditions. In addition, P5.2 inhibits keratinocyte multiplication, a favorable result for its applicability in actinic keratosis.

Chapter 4. Complex study for the selection of tetrapyrrole molecules with applicability in the therapy of premalignant and malignant skin disorders

Another stage in the development of the experimental part of the doctoral thesis was the selection of tetrapyrrolic compounds with photosensitizer potential in the therapy of premalignant and malignant skin disorders. Five compounds with a porphyrinic structure (Figure 4.1.) were evaluated based on structural, spectral and pharmaco-toxicological criteria (Boscencu et al., 2017; Boscencu et al., 2020; Boscencu et al., 2023):

- *5,10,15,20-tetrakis-(4-acetoxy-3-methoxyphenyl) porphyrin (**P2.1**)*
- *5-(4-hydroxy-3-methoxyphenyl)-10,15,20-tris-(4-acetoxy-3-methoxyphenyl) porphyrin (**P2.2**)*
- *5,10,15,20-tetrakis-(4-carboxymethylphenyl) porphyrin (**P3.1**)*
- *5-(2-hydroxy-5-methoxyphenyl)-10,15,20-tris-(4-carboxymethylphenyl) porphyrin (**P3.2**)*
- *5-(2,4-dihydroxyphenyl)-10,15,20-tris-(4-acetoxy-3-methoxyphenyl) porphyrin (**P4.2**)*

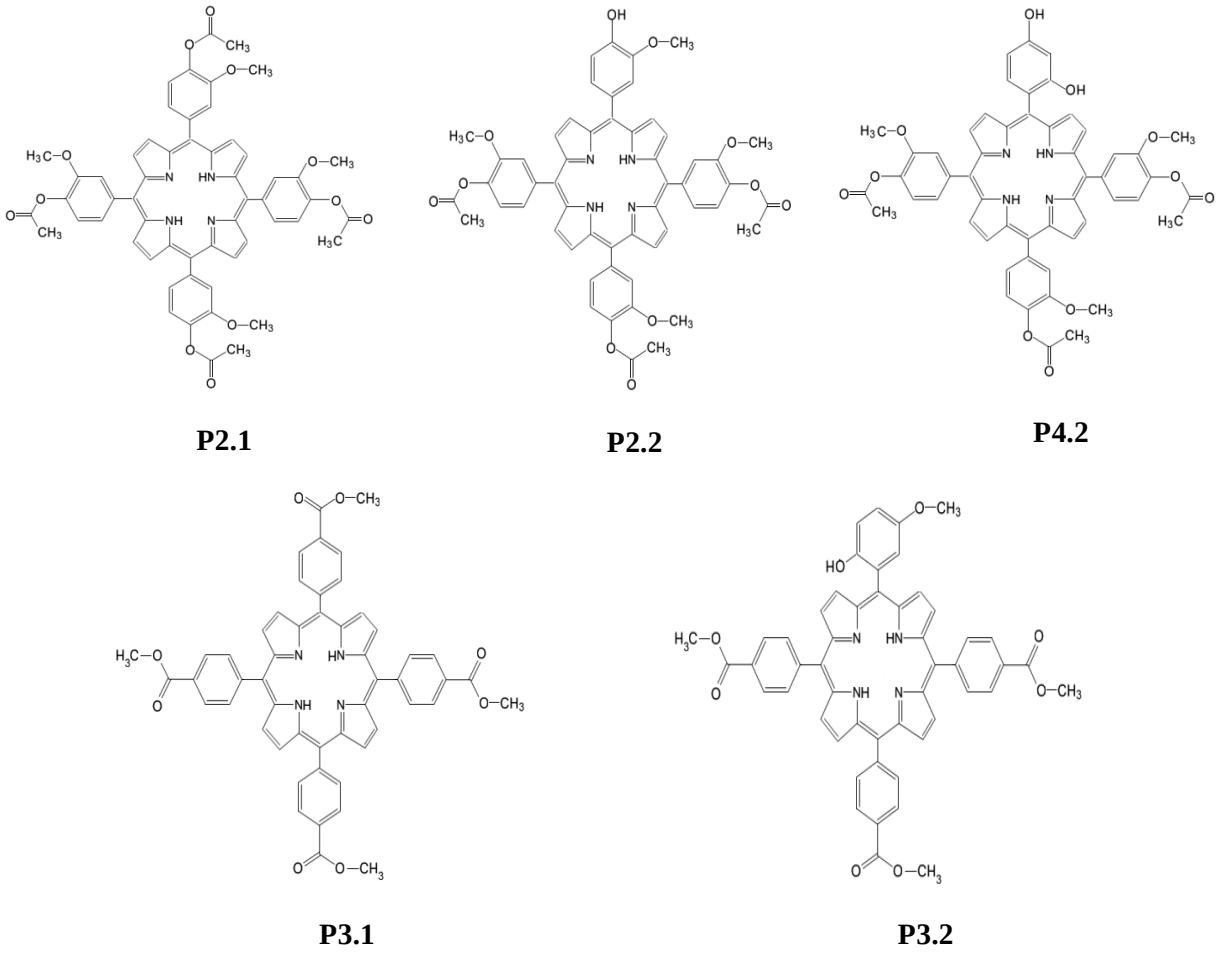

P2.1 **P2.2** **P4.2**

P3.1 **P3.2**

Figure 4.1. The molecular structure of the investigated porphyrins

The study aimed to:

- the *in silico* analysis regarding to the diffusion potential through the cell membrane of the porphyrinic compounds and the prediction of their ADMET (absorption, distribution, metabolism, elimination, toxicity) profile;

- evaluation of the molecular aggregation potential in 10 µM solutions (PEG 200 solvent);
- analysis of the spectral profile of porphyrins in 10 µM solutions with PEG 200 or PBS solvent;
- evaluation of the therapeutic potential and toxicological profile of porphyrins by *in vitro* testing on normal human dermal fibroblasts, normal human keratinocytes and tumor cell lines (squamous cell carcinoma and mouse melanoma). *In vitro* studies have looked at the ability to localize at the cellular level, the biocompatibility and the potential of the compounds to destroy tumor cells upon activation with light of specific wavelength (*in vitro* photodynamic therapy).

In silico analysis regarding to the diffusion potential through the cell membrane and the ADMET profile of the porphyrinic compounds included in the study

Since the cellular uptake of porphyrin derivatives is essential for acting as effective photosensitizers in cells and tissues, we first predicted the translocation of the investigated compounds through the cell membrane using the PerMM web-server (*Permeability of Molecules across Membranes*) (Lomize et al., 2019). The membrane transfers energy (ΔGtransf) profiles along with the lipid bilayer normal (Z) and the optimized spatial conformations for the investigated porphyrin derivatives are illustrated in Figure 4.2.

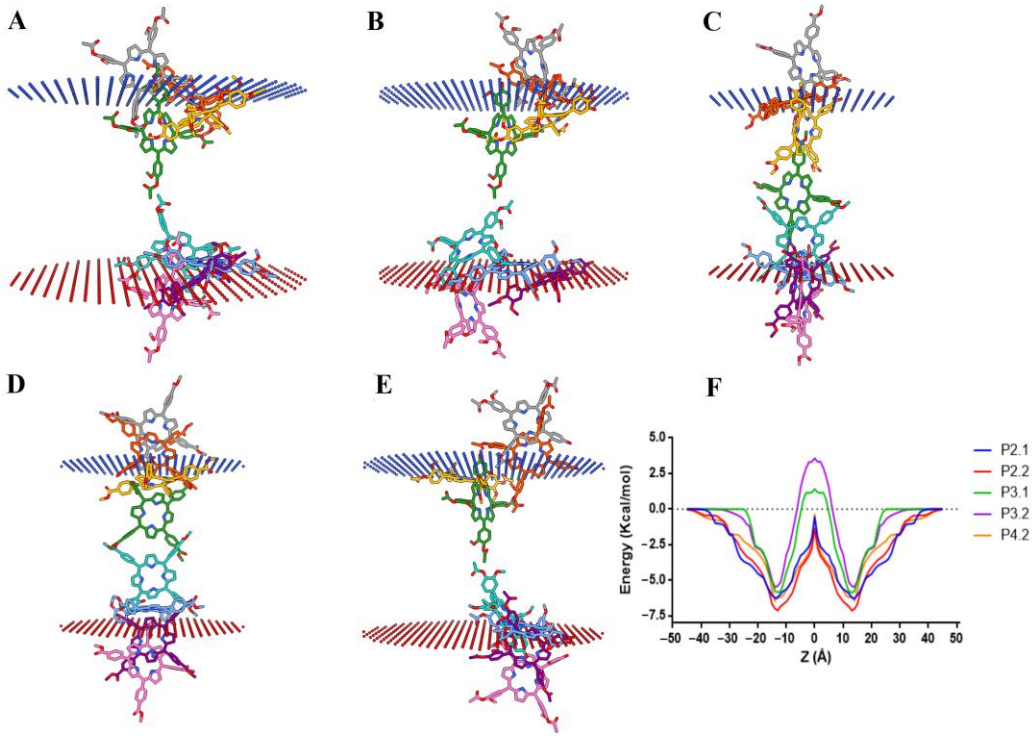

Figure 4.2. (**A**–**E**) Representative snapshots illustrating the predicted translocation pathways across the lipid bilayer for P2.1 (**A**), P2.2 (**B**), P3.1 (**C**), P3.2 (**D**), and P4.2 (**E**); (**F**) Variation of the transfer energy (ΔG_{transf}) as a function of distance from the center of the lipid bilayer (Z) (Burloiu et al., 2024a).

The porphyrinic compounds P2.2, P4.2, and P2.1 were highly likely to permeate the cell membrane according to the calculated LogPerm values and the $\Delta G_{transf}(Z)$ profiles, while the translocation of P3.1 and P3.2 could be achieved with increased difficulty, requiring higher transfer energies, although P3.2 had the potential to interact with the hydrophilic heads of membrane lipids through hydrogen bonding (Burloiu et al., 2024a). Several pharmacokinetic and toxicological properties were predicted for the investi- gated compounds using three web-servers: admeSAR (Yang and colab., 2019), pkCSM (Pires et al., 2015) și ProTox-II (Banerjee et al., 2018). Considering that the porphyrin derivatives were designed for topical administration in skin disorders, the most relevant ADMET properties are skin permeability and skin sensitization. All the porphyrin derivatives had the same value for the predicted logarithmic skin permeability (log Kp, −2.735 cm/h), which falls within the acceptable range for drugs (Chavan et al., 2014). The predicted subcellular localization was the mitochondrion, which could improve the efficacy of PDT. The investigated compounds had a relatively low predicted toxicity (class V) and were negative regarding skin sensitization (Burloiu et al., 2024a).

Atomic force microscopy assessment of the molecular aggregation potential of porphyrinic compounds in PEG 200

AFM has proven to be a versatile method in assessment of the structural profile and molecular aggregation potential of porphyrins with applicability in PDT. The method provides information on the morphology and textural properties of the tetrapyrrolic structures and allows the assessment of the molecular aggregation capacity, a phenomenon with a major influence on the cellular behavior of these compounds. Therefore, the complex study for selection of porphyrins with potential applicability in PDT for premalignant and malignant skin disorders, also included the evaluation by AFM of the aggregation status of structures P2.1, P2.2, P3.1, P3.2 and P4.2. The results of the experimental study are presented in the reference Burloiu et al. 2024a. Atomic force microscopy (AFM) measurements were performed in non-contact mode as recommended for soft samples, using the XE-100 model from Park Systems (Suwon, Republic of Korea) and 10 µM porphyrinic solutions (PEG 200 solvent). Enhanced-color bi-dimensional (2D) topographic AFM images of the samples P2.1, P2.2, P3.1, P3.2, and P4.2 in PEG 200, scanned over an area of (10 10) μm^2, were obtained, together with characteristic surface profiles (line scans) (Figure 4.3). Based on AFM investigations at the scale of (10x10) μm^2, it was found that all investigated samples were isotropic and self-similar, with slightly different degrees of aggregation. P2.1 had the highest aggregation tendency (Figure 4.3.a).

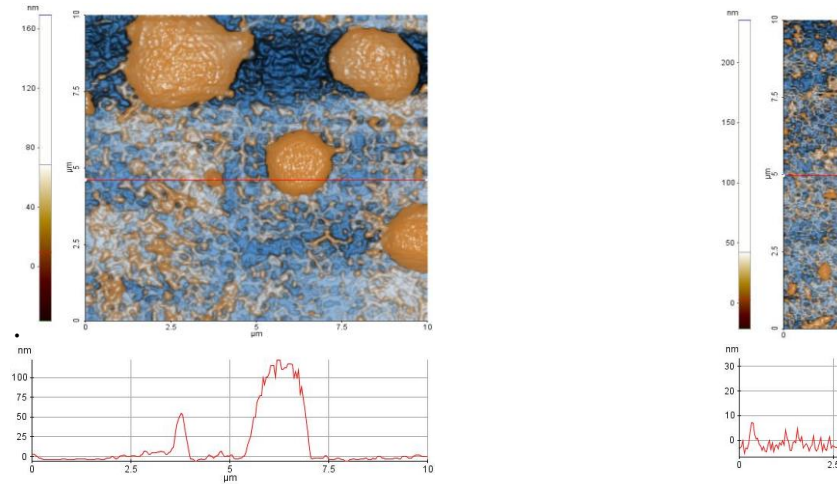

(**a**)

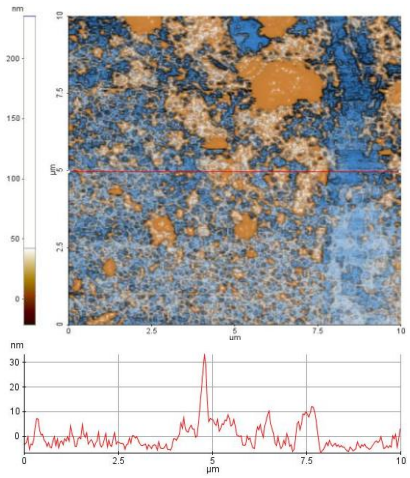

(**b**)

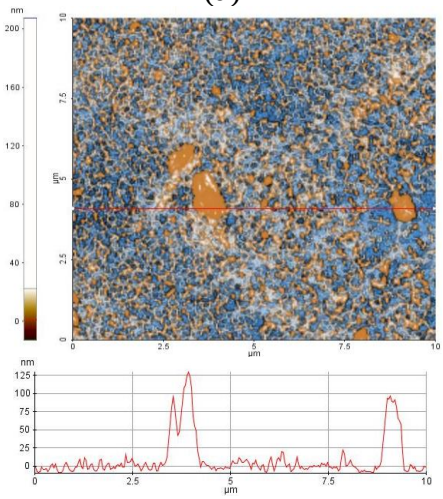

(**c**)

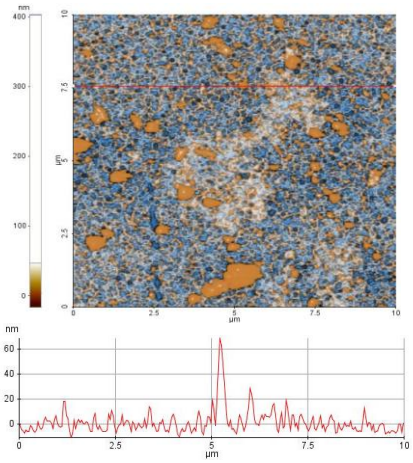

(**d**)

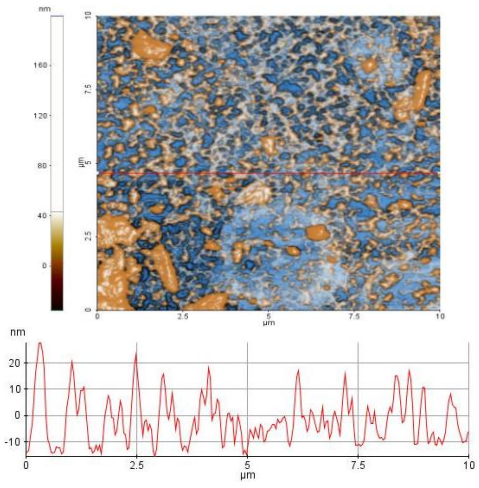

(**e**)

Figure 4.3. Enhanced contrast bi-dimensional (2D) topographic AFM images of samples P2.1 (**a**), P2.2 (**b**), P3.1 (**c**), P3.2 (**d**), and P4.2 (**e**), scanned over an area of (10×10) μm^2, together with random cross-sectional height examples (line scans).

Study of the UV-Vis and fluorescence spectral behavior of some solutions with 10µM porphyrin dissolved in PEG200 or PEG 200/PBS (1/1000)

The spectral behavior of the porphyrinic structures was assessed by UV-Visible and fluorescence spectroscopy. The UV–Vis spectra of the porphyrins were registered with a Specord 200 spectrophotometer (Analytik Jena, Jena, Germany). Fluorescence spectra were registered using a steady-state Jasco FP 6500 spectrofluorometer (JASCO Co., Ltd., Kyoto, Japan) (λ_{ex}= 410 nm). The stock solutions of porphyrins (10 mM) were prepared in PEG 200, and were further diluted for experiments to 10 µM in PEG 200, PEG 200/PBS (1/1000), or in cell culture medium, depending on the type of experiment. Because of their structural configurations, these compounds have demonstrated an excellent solubility in biologically friendly media, and long-term stability in PEG 200, a non-toxic and green pharmacologically accepted solvent.

At the concentration of 10 µM porphyrin, the molecular absorption spectra of the compounds P2.1, P2.2, P3.1, P3.2, and P4.2 had the typical profile of porphyrinic compounds, and did not indicate molecular association phenomena (Figure 4.4).

In the spectral range 400–407 nm, the Soret band was highlighted as a result of an intense absorption, and the Q bands were identified in the spectral region of 495–629 nm. The presence of the absorption maximum associated with the band Qx(0,0) at 621–630 nm confirmed the fact that the investigated porphyrin compounds absorbed in the phototherapeutic range (Pandey & Zheng, 2000; Simpson & Novikova, 2022). Small changes in the positioning of the absorption maxima were evidenced (Figure 4.4) as an effect of the structural differences between the tested compounds.

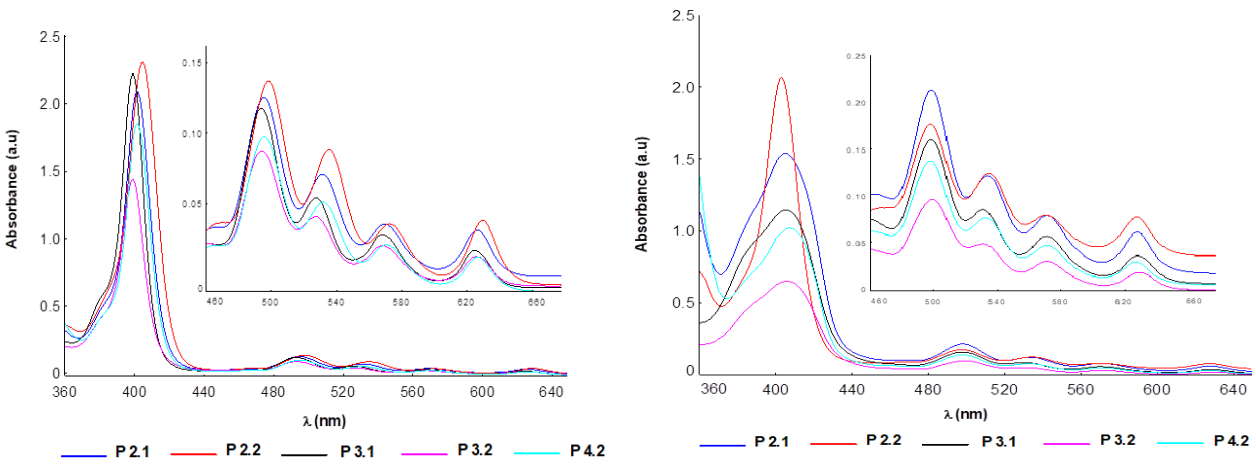

Figure 4.4. Absorption spectra of porphyrins (10 µM) dissolved in PEG 200 (**a**) and 10 µM dissolved in PEG 200/PBS (1/1000) (**b**).

Thus, the spectral bands of the asymmetric compounds were slightly shifted towards the red compared to those of the symmetric structures in the same solvent. Regarding the intensity of the absorption bands, the highest values of the molar extinction

coefficients were associated with compound P2.2, and the smallest with porphyrin P3.2 (Figure 4.4). Compared to the spectral region of therapeutic interest (621–630 nm), the best absorptions were registered for the P2.2 and P2.1 compounds (Figure 4.4).

According to published data (Gouterman, 1978; Gouterman et al., 1963), the changes found in the intensities and positions of the spectral bands are the consequence of: (i) the different structure of the functional groups attached to the porphyrinic macrocycle, and (ii) the energy values that accompany the electronic transitions between the orbitals fully occupied with electrons (a2u and a1u) and the unoccupied orbitals (e1g). Due to the nature of the peripheral substituents of the tetrapyrrole macrocycle, the P2.1, P2.2, and P4.2 compounds had a higher electronic charge compared to P3.1 and P3.2. Conjugation effects may appear between the electrons of these substituents and the electrons of the a2u orbitals, leading to an increased absorption intensity (Figure 4.4). In turn, the presence of two –OH functional groups in the structure of P4.2 increased the potential for hydrogen bonds formation with the solvent molecules, consequently decreasing the absorption intensity as compared to P2.2 and P2.1. The spectral profile of the investigated porphyrins did not change significantly in solutions with a content of 10 μM porphyrin in PEG 200/PBS (1/1000), as compared to porphyrin solutions in PEG 200 (Table 1). Nevertheless, a slight increase in the absorption intensity, accompanied by small bathochromic shifts of the spectral bands, was highlighted (Figure 4.4b).

The emission properties of the investigated compounds were influenced by the nature of the solvent and the electronic effects dictated by the structural particularities of each porphyrin. For the same solvent, the emission spectra of the investigated porphyrins kept the spectral profile typical of the fluorescence of free base porphyrins, with a decrease in fluorescence in the order P2.1 > P3.1 > P2.2 > P4.2 > P3.2 (Figure 4.5). Regarding the fluorescent properties of the investigated compounds at a concentration of 10 μM porphyrin in PEG 200/PBS (1/1000), small shifts of the spectral bands were observed, with a decrease in fluorescence intensity (more for P3.1, P2.2, and P4.2) compared to porphyrin solutions of the same concentration in PEG 200. These spectral changes might be due to the formation of molecular associations through physical interactions when using the PEG 200/PBS solution as solvent, which produces fluorescence extinction. Regardless of the nature of the solvent, the symmetric structures P2.1 and P3.1 exhibited higher fluorescence than the asymmetric ones (P2.2, P4.2, P3.2). The decrease in the fluorescent signal was a consequence of the electronic effects induced by the –OH functional group, and of displacements of the electron density in the π-conjugated systems of the porphyrinic structure. As an example, the P2.2 and P4.2 asymmetric structures had weaker fluorescence as compared to the symmetrical structure P2.1.

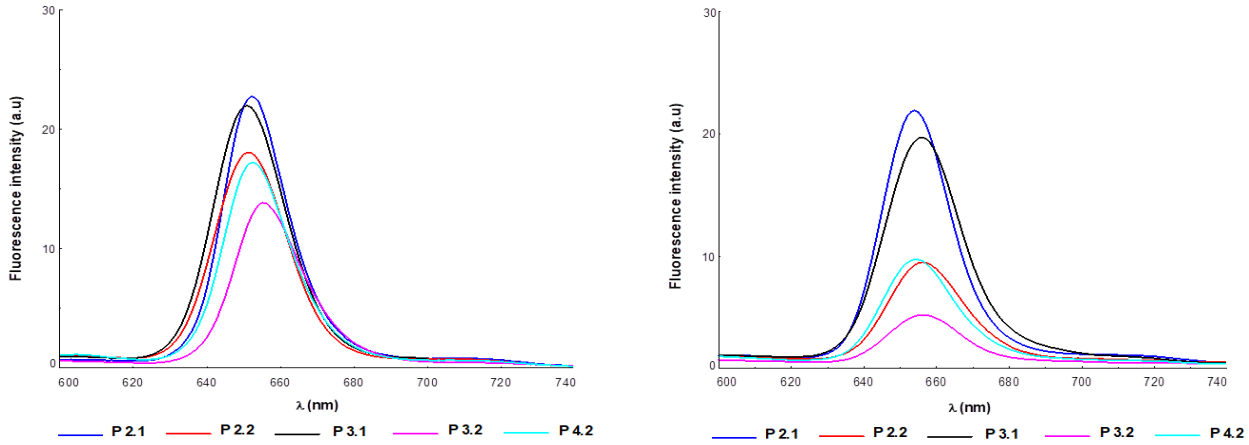

Figure 4.5. Emission spectra of porphyrins at a concentration of 10 µM in PEG 200 **(a)** and PEG 200/PBS (1/1000) **(b)** as solvent. λex = 410 nm.

Concluding, under the experimental conditions addressed, the investigated compounds confirmed absorption in the expected range relevant for PDT. Furthermore, emission spectra had the typical profile of the spectrum associated with a porphyrinic photosensitizer, with small shifts of the emission maxima in the case of the porphyrin solutions in PEG 200/PBS (1/1000).

Selection of porphyrin photosensitizers by assessment of cellular internalization potential and therapeutic profile. In vitro testing on normal human dermal fibroblasts, normal human keratinocytes and tumor cell lines

The cellular uptake of compounds and the effect of photodynamic therapy on the viability, proliferation, and necrosis of human HaCaT keratinocytes, human Hs27 skin fibroblasts, human skin SCL II squamous cell carcinoma, and B16F10 melanoma cells were assessed in vitro, in correlation with the structural and photophysical properties of the investigated porphyrins, and with the predictions regarding diffusion through cell membranes and ADMET properties.

Porphyrins were investigated in cellular systems using standardized cell lines purchased from ATCC (Manassas, VA, USA)—Hs27 fibroblasts from human foreskin, and B10F10 murine melanoma cells, and from CLS Cell Lines Service GmbH (Eppelheim, Germany)—HaCaT spontaneously immortalized keratinocytes from adult human skin, and SCL II squamous cell carcinoma cell lines from face skin. The experimental methodology applied in the *in vitro* studies is detailed in the reference Burloiu et al. 2024a.

Cellular Uptake of the Investigated Porphyrins

For assessing the cellular uptake of porphyrins, we took advantage of their fluorescent properties and measured by flow cytometry the mean fluorescence of cells suspended in PBS. Cells were incubated in the previous 24 h with porphyrins at 10 µM concentration in culture medium.

Considering that the investigated compounds had different intensities of the emission peak, the measured intracellular fluorescence was normalized to the corresponding maximal fluorescence intensity of each porphyrin, for having reliable data on cellular uptake, independent of the fluorescent properties of each porphyrin. Nevertheless, we did not take into account the potential decrease of the intracellular fluorescent signal due to the interaction of porphyrins with intracellular components. According to the flow cytometry data (Figure 4.6), P2.2 had the best uptake in all the investigated cell lines ($p < 0.05$), followed by P3.2, P4.2, and P2.1 (symmetrical compound).

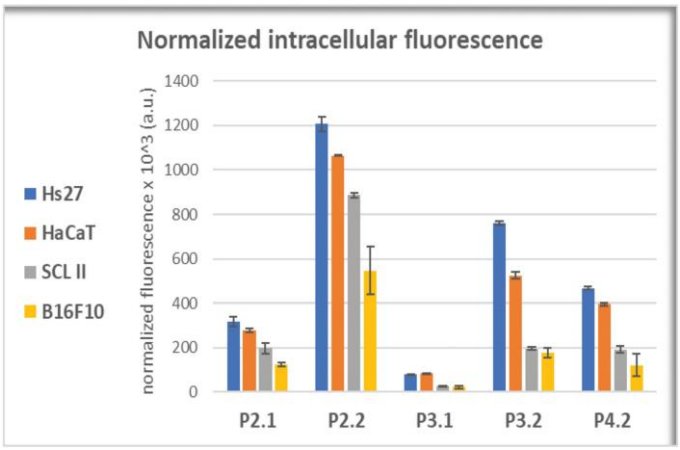

Figure 4.6. Intracellular fluorescence of porphyrins (24 h incubation of porphyrins, 10 µM) with skin-relevant cells: Hs27, HaCaT, SCL II and murine B16F10 melanoma cells. Intracellular fluorescence was assessed by flow cytometry as geometric mean of the fluorescence signal normalized to the corresponding fluorescence emission of the porphyrin in PEG 200/PBS (1/1000) as solvent. Data are presented as mean value ± SD for 2–3 independent experiments in which all porphyrins were investigated simultaneously.

The lowest incorporation into cells was registered for the P3.1 compound, a result matched to the computational study which showed that P3.1 and P3.2 required high, positive transfer energies to permeate across the membrane core, higher energy values being also registered at the water–lipid interface. Although P3.2 was predicted through computational methods to have the lowest uptake, this was not confirmed by the in vitro study. For all the investigated porphyrins, the uptake was higher in normal fibroblasts and keratinocytes, while lower values were registered in SCL II and B16F10 tumor cells, with P2.2 having the best incorporation profile into cells, either

non-malignant or malignant (Figure 4.6). Although the symmetrical P2.1 compound had the best fluorescent properties, (Figura 4.5), its incorporation in cells was significantly lower than that of the asymmetric P2.2 compound in terms of intracellular fluorescence, probably due to its higher aggregability, as shown by the AFM measurements (Figure 4.3a). Altogether, results indicate that, from the point of view of cellular uptake, the asymmetric P2.2 porphyrin is most suitable for incorporation in non-malignant or malignant skin cells, with best results in normal cells

In Vitro Effects of Photodynamic Therapy with Investigated Porphyrins

The ability of the investigated porphyrins to kill cells by PDT was investigated in vitro on human skin-relevant cell lines: Hs27 fibroblasts, HaCaT keratinocytes, and SCL II squamous cell carcinoma cells. Mouse B16F10 melanoma cells were also investigated for comparison. After incubating cells with porphyrins (10 μM) for 24 h, PDT was performed using laser light of 635 nm, at fluences previously communicated by us (10 J/cm^2, 50 mW/cm^2) (Dobre et al., 2021). After PDT, cells were cultivated for another 24 h or 48 h for establishing the impact of PDT at the level of MTS reduction, which provides information on the number of metabolically active cells, and of lactate dehydrogenase (LDH) release, which assesses the disturbance of the plasma membrane integrity due to cell death by necrosis. The MTS reduction data (Figure 4.7) showed that P2.2 and, to a slightly lesser extent, the symmetrical P2.1 compound induced a drastic decrease in the number of metabolically active cells at 24 h, the effect being persistent also at 48 h after PDT. The effect of porphyrin P4.2 depended on the cell-type. Thus, P4.2 decreased the intensity of MTS reduction in Hs27 fibroblasts exposed to PDT, at levels similar to those elicited by PDT with the symmetrical P2.1 compound, and only modestly decreased the number of metabolically active HaCaT keratinocytes, SCL II squamous cell carcinoma cells, and B16F10 melanoma cells as compared to P2.1, especially at 24 h. Meanwhile, we did not register a consistent decrease in MTS reduction in any of the investigated cell lines exposed to PDT with P3.1 and P3.2, although P3.2 was well incorporated by the investigated cells, especially by fibroblasts and keratinocytes.

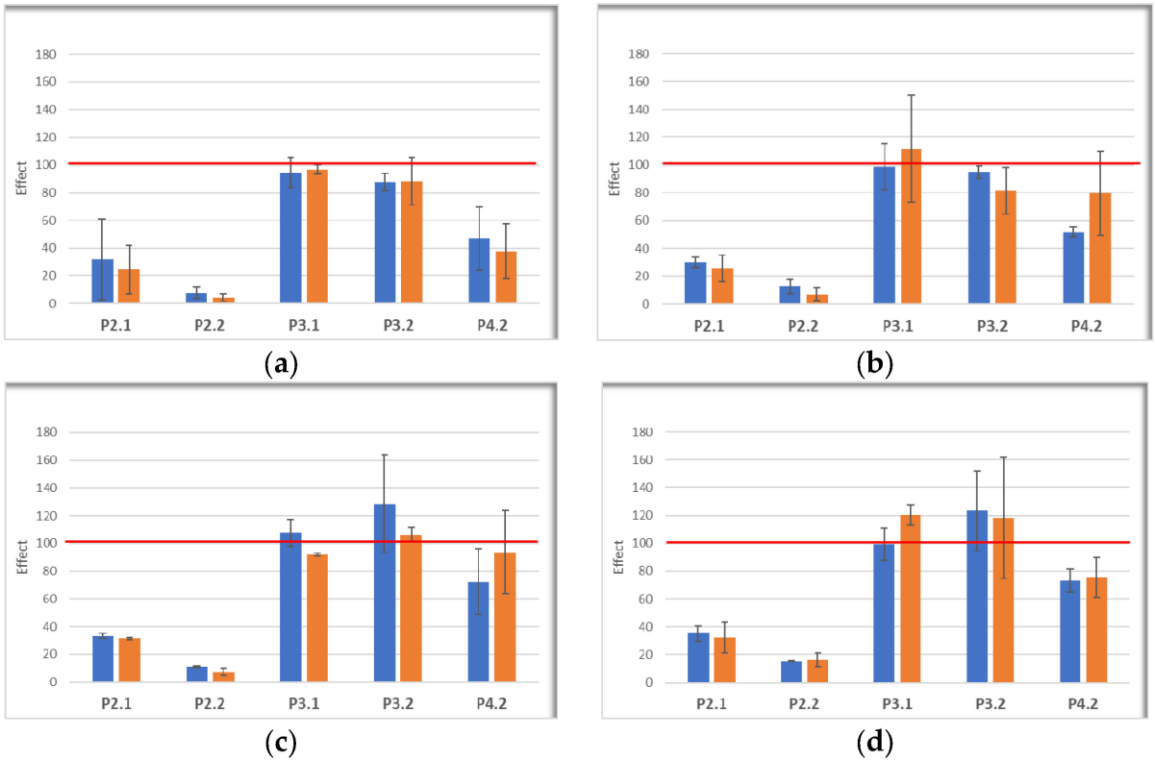

Figure 4.7. The MTS reduction by skin cells Hs27 (a), HaCaT (b), SCL II (c) și B16F10 (d), incubated with porphyrins (10 μM), and thereafter exposed to PDT (10 J/cm^2, 50 mW/cm^2). Measurements were performed at 24 h (blue) and 48 h (orange) after PDT. The effect of PDT on MTS reduction was calculated as: (cellular response in the presence of PDT)/(cellular response in the absence of PDT) × 100. Red line designates the 100% effect (no effect).

For investigating cell death by necrosis following PDT, LDH release was measured in the same cellular samples in which MTS reduction was assessed. LDH release (effect > 500%) was registered within the first 24 h after PDT in Hs27 fibroblasts and HaCaT keratinocytes exposed to PDT with the P2.1, P2.2, and P4.2 compounds (Figure 4.8a,b), indicating that the decrease in metabolically active cells after PDT was partly due to rapid cell death by necrosis. The LDH release response was smaller in the case of tumor cells (Figure 4.8c,d), for which the effect of PDT on MTS reduction was also low (Figure 4.7). While an increased LDH release was confined to the first 24 h after PDT in the case of P2.1 and P2.2, cell death by necrosis continued to occur also at 48 h in the case of PDT with P4.2. Meanwhile, no significant increase in LDH release was registered when PDT was performed with the P3.1 and P3.2 compounds, for which MTS reduction also had nonsignificant changes (Figure 4.7). Altogether, results point to the asymmetric P2.2 porphyrin as a valuable candidate for PDT in malignant skin disorders, with the amendment that normal skin around the tumor should be protected from PDT.

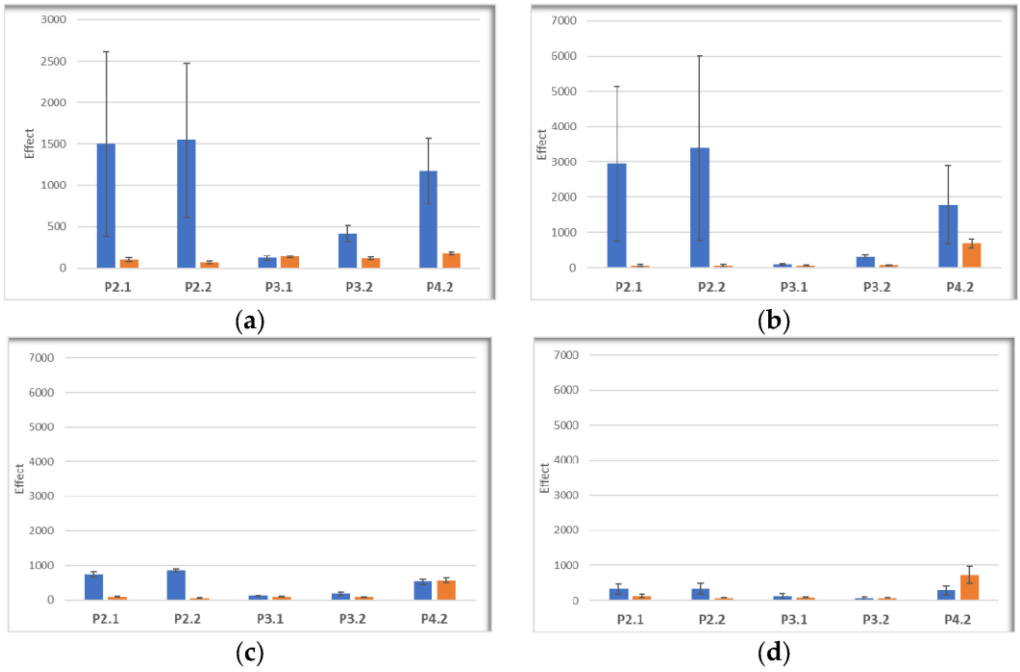

Figure 4.8. LDH release by cells Hs27 (a), HaCaT (b), SCL II (c) și B16F10 (d), incubated with porphyrins (10 μM), and thereafter exposed to PDT (10 J/cm^2, 50 mW/cm^2). Measurements were performed at 24 h (blue) and 48 h (orange) after PDT, in the same cellular samples in which MTS reduction was assessed. The effect of PDT on the LDH release was calculated as: (cellular response in the presence of PDT)/(cellular response in the absence of PDT) × 100. Results are presented as mean effect ± SD for 2–3 independent experiments.

The *in vitro* study performed on non-malignant and malignant skin-relevant cells highlighted that the asymmetric P2.2 porphyrin qualified among the five investigated porphyrins to be a promising photosensitizer candidate for PDT in skin disorders. P2.2 was shown to accumulate well within cells, although it hada certain degree of aggregation in PEG 200, and induced by PDT a massive decrease in the number of metabolically active skin cells, partly due to cell death by necrosis within the first 24 h post-PDT. P2.2 had in this respect a better behavior than the symmetric P.2.1 compound which, albeit exhibiting the best fluorescent properties, had a higher degree of aggregation. P2.2 was also superior to the related asymmetric compound P4.2. The P3.1 and P3.2 compounds had a predicted high value of total clearance, and were not able to accumulate well in skin cells, although they exhibited a lower degree of aggregability than P2.2, and did not elicit significant PDT in vitro consequently.

Chapter 5. Formulation studies of selected photosensitizers for applications in dermato-oncology

Studies on the formulation of selected photosensitizers for applications in dermato-oncology, followed the incorporation of P2.1 and P2.2 porphyrins into hydroxypropylcellulose (HPC), hydroxypropylmethylcellulose (HPMC) and Carbopol 940 hydrogels. Their spectral and structural evaluation was carried out by UV-Vis and fluorescence analysis, FTIR, X-ray diffraction, thermo-gravimetric analysis, atomic force microscopy. Additionally, pharmacotechnical evaluations were performed to assess the mechanical properties, pH, swelling ratio, and spreadability of the gels, aiming to establish their suitability for biomedical applications in PDT.

In a first stage, 10% HPC, 10% HPMC and 1% Carbopol hydrogels were obtained by dispersing polymer into water and their mixing at 800 rpm at room temperature. For deaerating, the hydrogels were kept overnight in the fridge at 5°C. In the case of the gel with Carbopol, after 24 h triethanolamine was added, gradually and under continuous stirring until a translucent gel was obtained. The obtained gels served as a references in the subsequent analyses and also as a base for the studied porphyrins' gels. In total, 1 g of each 1mM porphyrin solution in PEG 200 was separately added to 49 g of base gel and stirred in the dark at 750 rpm and at room temperature. The properties of the obtained gels were evaluated in comparison to the simple 10% hydrogels.

Pharmacotechnical evaluation showed that the hydrogels have suitable mechanical properties for application on the skin. The pH of the hydrogels was found to be within the optimal range for topical applications, minimizing the risk of irritation. Furthermore, good water absorption capabilities were observed, which are beneficial for maintaining a moist wound environment. An excellent spreadability was also noted, ensuring easy application and even coverage on the skin surface.

Physicochemical evaluation of hydrogels with porphyrins

The results of the UV-Vis and fluorescence analysis highlight the maintenance of the spectral profile of the two porphyrins after incorporation into polymer gels, with the maintenance of absorption and emission maxima in the spectral range relevant for applications in PDT (Simpson & Novikova 2022). The absorption and fluorescence maxima of the investigated samples are presented in table 5.1. Also, in figure 5.1, the absorption and emission spectra of P2.1 and P2.2 in the HPMC matrix, are shown as examples.

Table 5.3. Spectral characteristics of porphyrin gels

Gel	Absorbtion λ_{max} (nm)					Emision λ_{max}(nm)
	Soret Band	Qy(1,0)	Qy(0,0)	Qx(1,0)	Qx(0,0)	
HPC-P2.1	427	517	551	589	647	653
HPMC-P2.1	426	518	552	591	658	654
Carbopol-P2.1	427	516	550	595	645	652
HPC-P2.2	426	517	556	597	649	654
HPMC-P2.2	428	521	556	594	652	656
Carbopol-P2.2	424	519	555	590	650	654

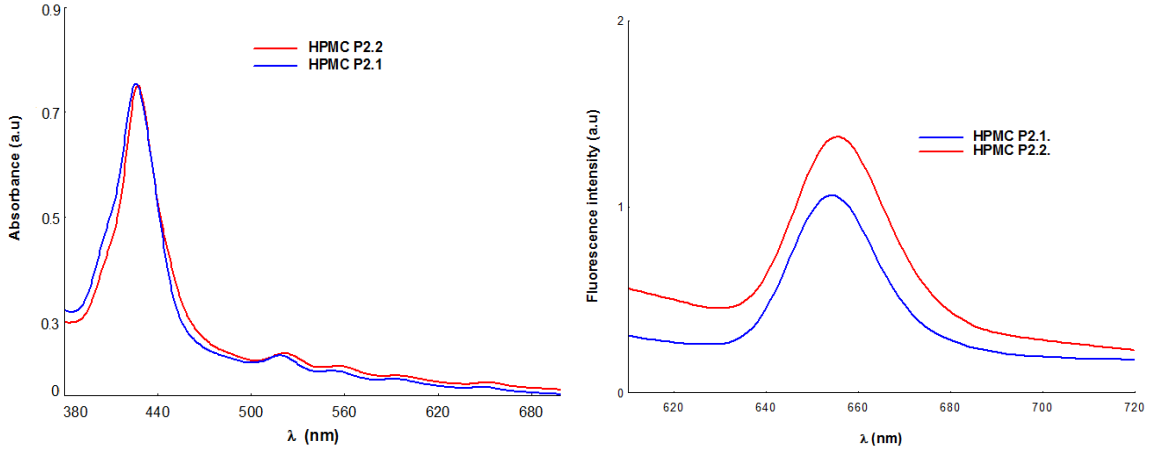

(a) **(b)**

Figura 5.1. Absorption **(a)** and fluorescence **(b)** spectra of gels with porphyrins in HPMC polymer matrix

The FTIR spectra confirmed incorporation of porphyrins into the polymeric matrix, by characteristic absorption bands which suggests interactions porphyrin-polymer type. In Figure 5.2, the FTIR spectra of the gels from the HPC series are shown. A slight shift and a small change in the intensity of the peak from 3400 cm^{-1} due to the interaction between the -OH groups of HPC and the two porphyrins (3401.82 cm^{-1} for HPC P2.1. and 3393.14 cm^{-1} for HPC P2.2.) was observed. The bands due to CH_2 and CH stretching also show small changes due to the polymer interaction with methoxy and acetoxy groups from P2.1. and P2.2 structure. Comparative analysis between the HPC P2.2. and HPC P2.1. gels indicate distinct interaction patterns. The presence of the -OH group in the structure of P2.2 gives the molecule a greater interaction potential with the polymer matrix than the compound P2.1, with effects on the spectral properties of the gel. Thus, in the case of HPC-P2.2, the FTIR signal associated with the –OH group shifts to lower frequencies (at 3393.14 cm^{-1}) compared to HPC-P2.1 (3401.82 cm^{-1}). Similar spectral changes were also highlighted for HPMC and Carbopol gels.

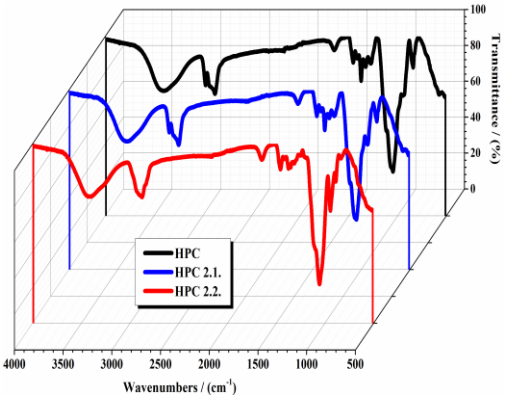

Figure 5.2. FTIR spectra of the gels from the HPC series

Morphological and textural profile assessment of porphyrin gels was performed by atomic force microscopy. AFM measurements were performed in "non-contact" mode with XE-100 (Park Systems, Suwon, Republic of Korea) equipped with decoupled sample/probe scanners, thus having a weak tip–sample interaction. The AFM figures are presented in the so-called "increased contrast" mode. The images were processed with the XEI program (v 1.8.0, Park Systems) for display purposes (tilt correction). Several roughness parameters were evaluated: from amplitude parameters, root-mean square roughness (Rq—the standard deviation of the height value in the image) and the peak-to-valley parameter (Rpv—the height difference between the lowest and the highest points in the surface); and, respectively, from the functional parameters, as reduced summit height (Spk—the height of the material in the peak zone), core roughness depth (Sk—the height difference between the intersection points of the found least mean square line), and the reduced valley depth (Svk—the height of the valley zone).

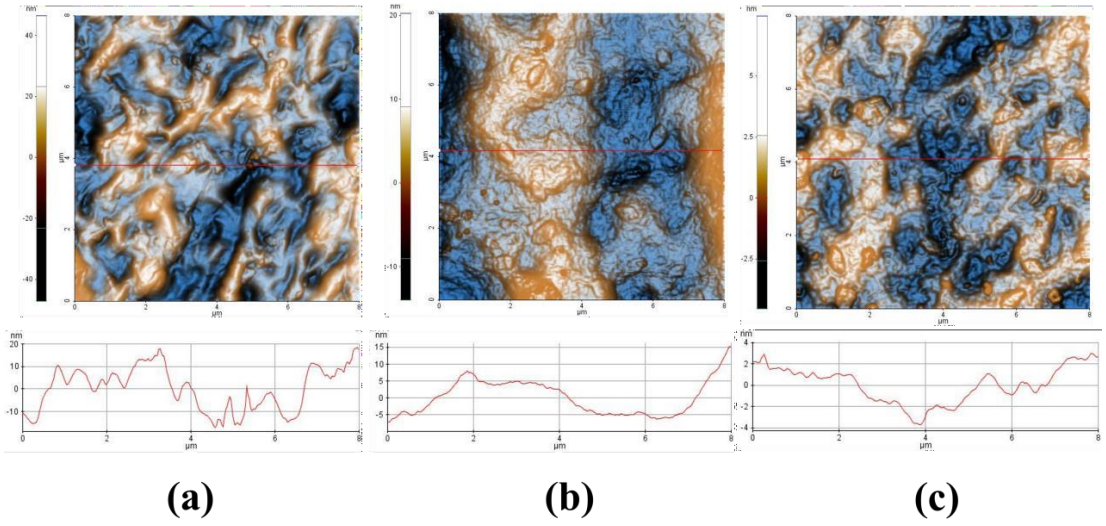

Figure 5.3. Two-dimensional AFM images, topography, at the scale of 8 µm × 8 µm of the 10% HPC (**a**), HPC P2.1. (**b**), and HPC P2.2. (**c**), accompanied by representative line scans, plotted at the position indicated in the AFM images by red horizontal lines.

Figure 5.3 shows the 2D topographic AFM images of the 10% HPC, HPC P2.1. and HPC P2.2. samples, scanned over an area of 8µm x 8µm. The 10% HPC sample is characterized by a Root Mean Square (RMS) roughness of 11.9 nm and a peak-to-valley height difference of 93.7 nm. The incorporation of the P2.1. porphyrin into the polymeric hydrogel with 10% HPC decreases the corrugation of the surface, as can be visually observed in the AFM image (Figure 5.3b), and the corresponding line scan (in which the vertical scale is of approx. 20 nm). The overall scanned area has an RMS roughness of ~4.6 nm and a peak-to-valley parameter of 34.3 nm. The incorporation of the P2.2. porphyrin into the polymeric hydrogel (Figure 5.3c) leads to a further decrease in the corrugation parameters. The RMS roughness of the whole AFM image from Figure 5.3c was 1.3 nm, and the peak-to-valley parameter was 12.0 nm.

Figure 5.4 presents the evaluation of different roughness values, evaluated from amplitude parameters (Root Mean Square roughness and Peak-to-Valley) and functional parameters (Reduced Summit Height (Spk), Core Roughness Depth (Sk), and Reduced Val- ley Depth (Svk)). It can be observed that all roughness parameters decrease in the sequence: HPC > HPC P2.1. > HPC P2.2.

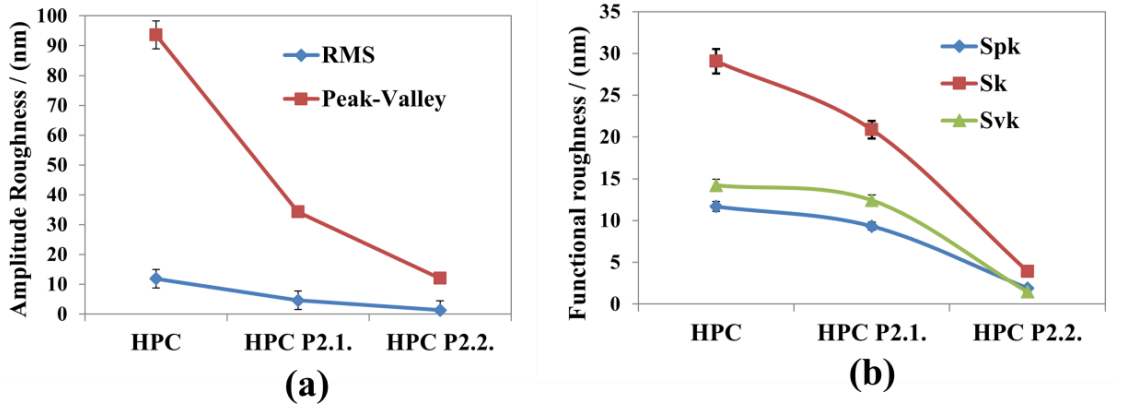

Figure 5.4. Roughness evaluation, 10% HPC, HPC-P2.1, and HPC-P2.2 samples based on Amplitude (RMS roughness and peak-to-valley) (**a**) and Functional parameters (Reduced Summit Height (Spk), Core Roughness Depth (Sk), and Reduced Valley Depth (Svk)) (**b**).

A high Sk value here correlates with the geometrical corrugation of the surface (larger Rq and RMS roughness values). Spk is related to a surface composed of high peaks that provide large areas of contact (stress) when the surface is contacted (HPC sample). In other words, the Spk parameter can represent the height of material that can be removed during friction. Svk is a measure of the valley depth below the core roughness, and can be related to possible liquid retention (or debris pickup). The lowest values in the series (sample HPC P2.2.) may express promising mechanical properties (pharmacotechnical applications). Similar determinations were also performed on HPMC and Carbopol gels; the obtained results confirmed the isotropic and self-similar texture for the surface of gels with porphyrins.

Thermogravimetric analyses were performed using Mettler Toledo TGA/SDTA851 thermogravimeter (Mettler-Toledo, Greifensee, Switzerland) under synthetic air flow at 80 mL/min with a heating rate of 10˚C/min.Thermogravimetric analysis provides crucial insights into the thermal stability and decomposition behavior of these types of materials. By comparing the thermal profiles of 10% gels with those of porphyrin gels it can understand how the presence of these porphyrins affects the thermal properties of the polymeric hydrogel systems. The thermal data obtained from TGA experiments are represented in Table 5.4.

Table 5.4. The thermal data obtained from TGA curves.

Gel	**1st Step** Temperature / Mass Loss	**2nd Step** Temperature	Remaining mass at 600˚C
HPC	< 100ºC/2.4%	T_{DTA} = 365ºC; T_{DTG} = 355ºC T_{DTA} = 495ºC; T_{DTG} = 501ºC	no residue
HPC-P2.1.	< 100ºC/1.8%	T_{DTA} = 367ºC; T_{DTG} = 357ºC T_{DTA} = 491ºC; T_{DTG} = 487ºC	no residue
HPC-P2.2.	< 100ºC/2.2%	T_{DTA} = 367ºC; T_{DTG} = 361ºC T_{DTA} = 492ºC; T_{DTG} = 489ºC	no residue
HPMC	< 100ºC/2.7%	T_{DTA} = 335ºC; T_{DTG} = 330ºC T_{DTA} = 461ºC; T_{DTG} = 458ºC	0.38%
HPMC-P2.1.	< 100ºC/2.2%	T_{DTA}=342.16ºC; T_{DTG}=345ºC T_{DTA}=453.8ºC; T_{DTG} = 453.5ºC	no residue
HPMC-P2.2.	< 100ºC/2%	T_{DTA}=342.6ºC; T_{DTG} = 346.5ºC T_{DTA} = 447ºC; T_{DTG} = 443ºC	no residue
Carbopol	< 150ºC/11.6%	T_{DTA}=206.3ºC; T_{DTG} = 205.3ºC T_{DTA} = 375ºC; T_{DTG} = 374.6ºC T_{DTA} = 528.1ºC;	3%
Carbopol-P2.1	< 150ºC/8.6%	T_{DTA} = 228ºC; T_{DTG} = 253ºC T_{DTG} = 447ºC; T_{DTG} = 443ºC	3.26%
Carbopol-P2.2	< 150ºC/10%	T_{DTA} = 240ºC; T_{DTG} = 233.1ºC T_{DTG} = 508ºC; T_{DTA} = 509.6ºC	2.9%

Figure 5.5 shows the thermal analysis curves of 10% HPC-based gels. The TG curve of 10% polymeric gels exhibits two main stages of weight loss: (i) in the first stage (below 100˚C for HPC, HPMC and below 150˚C for Carbopol), the initial weight loss is attributed to the evaporation of absorbed moisture and is in the range 2,4%-11,6%, indicating the loss of water physically bound to the polymer; (ii) the second stage which corresponds to the thermal degradation of the polymer backbone. The decomposition involves the breakdown of chemical linkages and subsequent volatilization of low molecular weight products. The thermal curves of porphyrinic gel displays a modified thermal profile compared to 10% polymeric gel. For all investigated samples, the first stage corresponds to moisture loss. The interactions

between polymeric gel and P2.1 and P2.2. affected the moisture retention capacity of the gel.

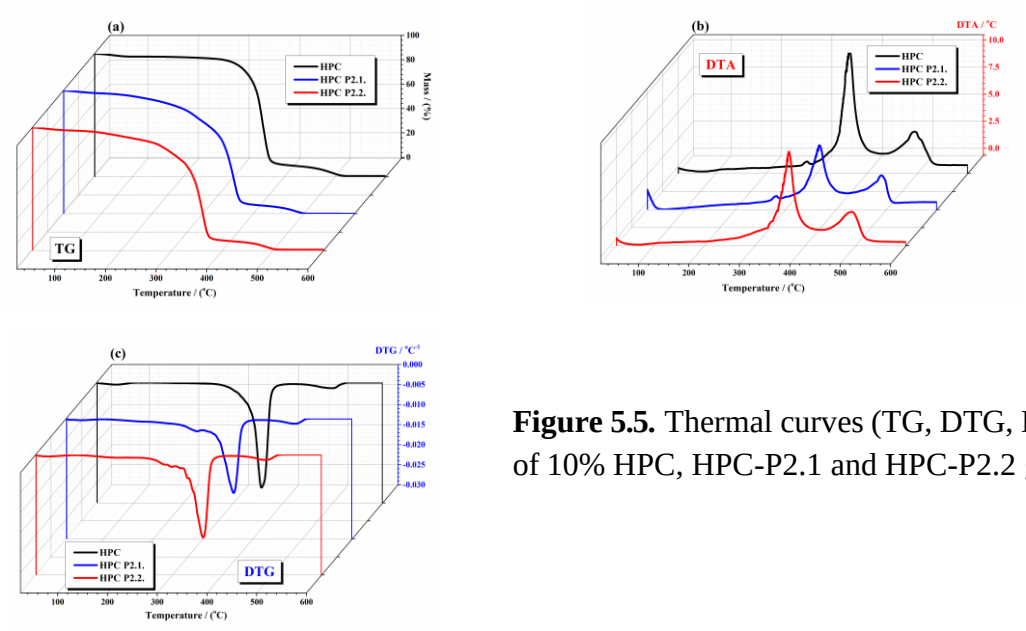

Figure 5.5. Thermal curves (TG, DTG, DTA) of 10% HPC, HPC-P2.1 and HPC-P2.2 gels

It was observed, in this stage, a weight loss of 1.8%- 2.2% for gels with porphyrins and cellulose derivatives. Gels with Carbopol registered losses of 8.6%-11.6%. Thermal analysis showed the thermal stability of the hydrogels in the temperature range relevant for pharmaceutical applications. Compared to the gel base, the thermal stability of gels with porphyrins is superior.

The surface morphology of the porphyrin gels was evaluated by the X-ray diffraction (XRD) analysis, using Rigaku Ultima IV diffractometer (Rigaku Co., Tokyo, Japan). The instrument operated in parallel beam geometry with CuKα radiation (λ = 1.5406 Å). XRD diffractograms were analyzed in the 2θ range of 5° to 60° at a scanning speed of 2°/min and a step size of 0.02°. An example of X-ray diffractograms for HPC series gels is shown in Figure 5.6.

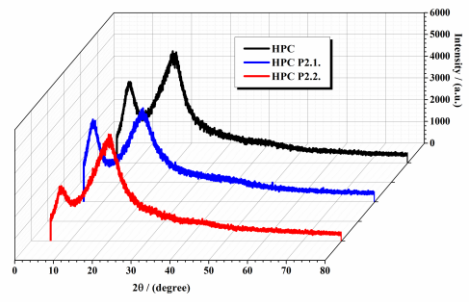

Figure 5.6. XRD diffractograms of 10% HPC, HPC-P2.1 and HPC-P2.2 gels

XRD analysis revealed that the porphyrins were effectively integrated into the HPC hydrogels, contributing to their stability and functional properties. The induced crystallinity, morphological and thermal properties of porphyrin gels suggest a good potential for PS release in topical PDT.

A final stage of the experimental part included an *in vitro* release study of P2.2 porphyrin from HPMC polymer matrix.

In vitro release studies were conducted using a Hanson Microette system (Hanson Research, Chatsworth, USA) equipped with vertical diffusion cells conforming to the United States Pharmacopeia guidelines (USP 2024). The receptor medium consisted of 20% (v/v) absolute ethanol in 0.05 M phosphate buffer (pH 6.0), prepared using ultrapure water. Supor® polyethersulfone (PES) membrane disc filters (25 mm diameter, 0.45 µm pore size, 145 µm thickness; Pall Life Sciences, Portsmouth, UK) were employed as the diffusion membrane. The gel formulation was carefully weighed and evenly applied onto the surface of the hydrated membrane in the donor compartment. The receptor medium was stirred continuously at 600 rpm At predetermined time intervals (30, 45, 60, 90, 120, 180, 240, 360 and 480 minutes), 1 mL samples were manually withdrawn from the receptor compartment in polypropylene Eppendorf tubes. The gel formulation was tested in sextuplicate (n = 6) and the results were expressed as mean values±standard deviation (SD). The concentration of porphyrin in the collected samples was determined using high-performance liquid chromatography.

A Jasco LC-4000 Series HPLC system (JASCO Corporation, Tokyo, Japan) was employed for the quantitative analysis of porphyrinic compound. The mobile phase consisted of water (mobile phase A) and a 1:1 (v/v) mixture of acetonitrile and methanol (mobile phase B). An isocratic elution was carried out with a mobile phase composition of 20% A and 80% B, delivered at a constant flow rate of 0.7 mL/min. Detection of porphyrin was performed at λ=419 nm, and the injection volume was 5 µL.

The method was validated according to the ICH Q2(R2) guidelines, (https://www.ema.europa.eu/en/documents/scientific-guideline/ich-q2r2-guideline-validation-analytical-procedures-step-5-revision-1_en.pdf . accessed on 12 June 2024).

By HPLC assay a linear response (R^2 = 0.9995) was observed over a porphyrin concentration range of 0.078–10 µg/mL, with the calibration curve defined by the equation y = 36662x - 4078. Assessment of assay specificity, conducted by evaluating potential interferences from the formulation matrix, confirmed the method's ability to accurately quantify P22 in the presence of excipients. The limit of quantitation, determined using a signal-to-noise ratio of 10:1, was established as 0.032 µg/mL.

The cumulative drug release per unit area over time is illustrated in Figure 5.9. The data represent the mean ± SD for six replicates. The system achieved equilibrium after 360 minutes, indicated by the plateau in the release profile. The release rate of P22 was determined using the Higuchi model, following the approach recommended by the SUPAC-SS guideline SUPAC-SS (https://www.fda.gov/media/71141/accessed on 12 June 2024).

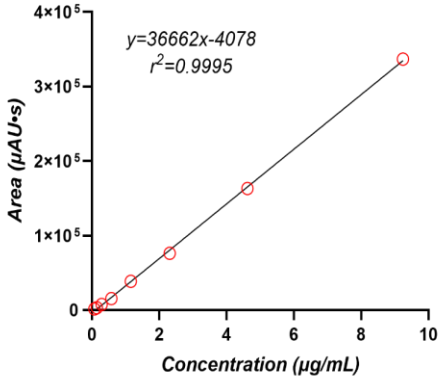

Figure 5.7. Calibration curve for P22 in the concentration range 0.078–10 µg/mL

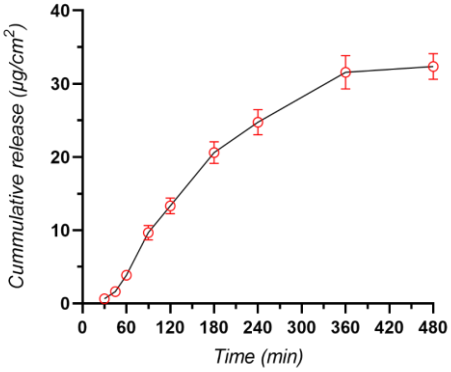

Figure 5.8. Cumulative amount of P22 diffused through the PES membrane plotted against time [min].

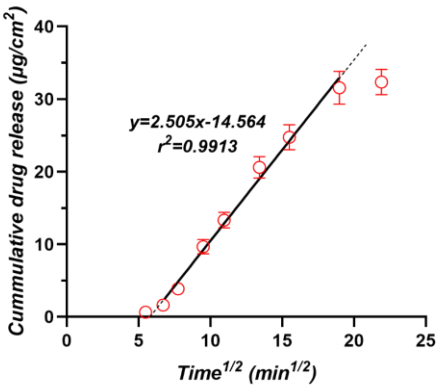

Figure 5.9. Cumulative amount of P22 diffused through the PES membrane plotted against square root of time [$min^{1/2}$].

The release rate was identified as the slope of the linear portion of the cumulative amount released plotted against the square root of time, corresponding to the achievement of steady-state transfer across the artificial membrane (Figure 5.9). This steady-state release was observed between 30 and 360 minutes. The calculated release rate was 2.505 µg/cm²/$min^{1/2}$, indicating a sustained release profile over the studied time frame. Additionally, an initial lag time of approximately 35 minutes was observed before the establishment of steady-state diffusion. During this phase, the drug molecules must overcome several barriers, including diffusion through the gel matrix and initial penetration of the membrane. The presence of this lag time suggests that the drug requires some time to saturate the membrane and build up a sufficient concentration gradient to drive steady-state diffusion.

GENERAL CONCLUSIONS

The PhD thesis "*Interdisciplinary studies on some tetrapyrrolic compounds with potential applicability in oncological dermatology*", includes in the first part a general presentation on the pathogenesis and therapy of premalignant and malignant skin disorders, supplemented by general data on Photodynamic Therapy as a modern therapeutic approach in oncological dermatology. The the basic principles of PDT and some examples of photosensitizers currently used in the treatment of malignant dermatological conditions are briefly presented.

The second part of the doctoral thesis is structured in three chapters that include the experimental results obtained in achieving the proposed objectives

In a first stage, we followed the synthesis, structural, spectral characterization and *in vitro* assessment of a new compound with potential applicability in oncological dermatology. In silico study results predicted for the porphyrinic structure, good membrane permeability with potential for localization at the mitochondrial level and good absorption in the skin. Docking and 250 ns molecular dynamics simulations confirmed for the chosen structure the ability to form a stable complex with the catalytic site of carbonic anhydrase IX, a target involved in cancer progression.

In chapter 3, the technical procedure for obtaining the new compound is described, specifying the associated parameters for synthesis and purification, and the results of its structural and spectral evaluation. Also, Chapter 3 includes the results of the evaluation of biocompatibility, cellular internalization capacity and fluorescent cell marker potential of porphyrinic compound. The *in vitro* experiments were completed by the study of the effects at the cellular level of the photodynamic therapy performed with the porphyrin derivative.

The *in vitro* assessment on cells relevant for premalignant and malignant skin conditions, revealed a good cellular internalization and a good biocompatibility for the tested compound. The good fluorescent profile and cellular incorporation capacity recommend P5.2 as a fluorescent marker in premalignant and malignant skin conditions. In addition, P5.2 inhibits keratinocyte multiplication, a favorable result for its applicability in actinic keratosis.

In chapter 4 of the PhD thesis, the results of the complex selection study of some porphyrinic structures with photosensitizing potential in PDT for premalignant and malignant skin diseases are presented. A strict evaluation based on structural, spectral and pharmaco-toxicological criteria allowed the selection of two porphyrins with an optimal profile for further formulation studies.

The in silico approach regarding the ability to cross the cell membrane revealed appreciable internalization potential for 3 of the investigated structures (P2.2, P4.2 and P2.1). The predictive models related to the ADMET profile associated with the

porphyrinic structures indicated relatively low toxicity for all compounds, being negative from the point of view of skin sensitivity.

The atomic force microscopy assessment of 10 µM porphyrin solutions (PEG 200 as solvent) allowed obtaining data on the aggregation status of these. For P2.1 porphyrin, the highest tendency of molecular aggregation was revealed.

Justified by the relevance of the spectral profile of a photosensitizer in terms of efficiency in PDT, the selection study included the evaluation of UV-Vis and fluorescent spectral behavior in 10µM solutions (PEG 200 or PEG 200/PBS (1/1000) as solvents). All investigated compounds have confirmed absorption in the phototherapeutic range (620–630 nm), spectral range relevant for photodynamic therapy.

The final selection of porphyrin photosensitizers was made by correlating the results obtained through the *in silico*, spectral and morphological evaluation with those regarding the localization potential at the cellular level and the effect of photodynamic therapy on normal and tumor cells specific to the skin.

The *in vitro* study performed on non-malignant and malignant skin-relevant cells highlighted that the asymmetric P2.2 porphyrin qualified among the five investigated porphyrins to be a promising photosensitizer candidate for PDT in skin disorders. P2.2 was shown to accumulate well within cells, although it had a certain degree of aggregation in PEG 200, and induced by PDT a massive decrease in the number of metabolically active skin cells, partly due to cell death by necrosis within the first 24 h post-PDT. P2.2 had in this respect a better behavior than the symmetric P.2.1 compound which, albeit exhibiting the best fluorescent properties, had a higher degree of aggregation. P2.2 was also superior to the related asymmetric compound P4.2. The P3.1 and P3.2 compounds had a predicted high value of total clearance, and were not able to accumulate well in skin cells, although they exhibited a lower degree of aggregability than P2.2, and did not elicit significant PDT in vitro consequently.

The complex study allowed the selection of compound P2.2 for the development of semi-solid pharmaceutical forms, effective for PDT in premalignant and malignant skin disorders. Justified by the good spectral profile and the appreciable therapeutic potential of P2.1, we included the two porphyrins P2.1 and P2.2 in the formulation studies of photosensitizers for applications in dermato-oncology.

Taking into account the fact that natural polymers offer the advantage of optimal bioavailability, are biocompatible, biodegradable and can ensure a good rate of transport of porphyrins to the tumor cell, in the formulation study of P2.1 and P2.2 we used hydroxypropyl cellulose as the gel base , hydroxypropylmethylcellulose and Carbopol 940.

UV-Vis and fluorescence spectral evaluation of the porphyrin gels confirmed the presence of the photosensitizer in the polymer matrix and the maintenance of its spectral characteristics within the range of interest for applicability in PDT. In addition, FTIR analysis revealed porphyrin-polymer hydrogen bonding interactions, suggesting the good potential of the chosen polymers as encapsulation matrices for porphyrins. Morphologically and texturally the gel formulations were evaluated by AFM, showing an isotropic and self-similar surface profile. Thermal analysis demonstrated the stability of the hydrogels in the temperature range relevant for pharmaceutical applications and XRD analysis confirmed the efficient integration of porphyrins into polymer gels, with relevant contributions to their stability and functional properties. The induced crystallinity, morphological and thermal properties of the porphyrin gels suggest a good photosensitizer release potential for use in topical PDT.

Preliminary *in vitro* release study performed with vertical diffusion cells, artificial membranes, receptor medium - absolute ethanol in phosphate buffer 0.05 M (20% (v/v) and pH=6), revealed a sustained release profile in the range of time studied.

In the experimental conditions addressed, the system reached equilibrium after 6 hours and the calculated release rate was 2.505 $\mu g/cm^2/min^{1/2}$, indicating a sustained release profile over the studied time frame.

The experimental results obtained through the complex evaluation of porphyrin gels are favorable for testing the biocompatibility and potential of PDT in relation to cell lines relevant for oncological dermatology.

Selected bibliography

1. Banerjee, P.; Eckert, A. O.; Schrey, A. K.; Preissner, R. ProTox-II: A webserver for the prediction of toxicity of chemicals. *Nucleic Acids Research*, **2018**, *46*(W1), W257–W263.

2. Boscencu, R.; Manda, G.; Radulea, N.; Socoteanu, R.P.; Ceafalan, L.C.; Neagoe, I.V.; Ferreira Machado, I.; Basaga, S.H.; Vieira Ferreira, L.F. Studies on the synthesis, photophysical and biological evaluation of some unsymmetrical meso-tetrasubstituted phenyl porphyrins. *Molecules* **2017**, *22*, 1815.

3. Boscencu, R.; Manda, G.; Socoteanu, R. P.; Hinescu, M. E.; Neagoe, I. V.; Olariu, L.; Dumitriu, B. Porphyrin Derivative for Theranostic Use. Patent No. 132752 B1: published in RO-BOPI, 11 from 29 November **2023 b.**

4. Boscencu, R.; Manda, G.; Olariu, L.; Neagoe, I. V.; Socoteanu, R. P.; Hinescu, M. E.; Vieira Ferreira, L. F.; Cuadrado, A.; Basaga, H. Tetrapyrrolic derivative for antitumor photodynamic therapy and obtaining process. Patent application 201900799, published in RO-BOPI, 9 from 30.09.2020.

5. Bray, F.; Laversanne, M.; Sung, H.; Ferlay, J.; Siegel, R. L.; Soerjomataram, I.; Jemal, A. Global cancer statistics 2022: GLOBOCAN estimates of incidence and mortality worldwide for 36 cancers in 185 countries. *CA Cancer J Clin*. **2024**, 74, 229-263.

6. Burloiu, A. M.; Manda, G.; Boscencu, R.; Neagoe, I.V.; Lupuliasa, D.; Surcel, M.; Olariu, L.; Mihai, D. P. *Porphyrinic compound with fluorescent marker potential in dermato-oncology*, Patent application 202200775/28.11.2022, published in RO-BOPI 5/30.05.2023.

7. Burloiu, A. M.; Manda, G.; Lupuliasa, D.; Socoteanu, R. P.; Mihai, D. P.; Neagoe, I. V.; Anghelache, L. I.; Surcel, M.; Anastasescu, M.; Olariu, L.; Gîrd, C. E.; Barbuceanu, S. F.; Ferreira, L. F. V.; Boscencu, R. Assessment of Some Unsymmetrical Porphyrins as Promising Molecules for Photodynamic Therapy of Cutaneous Disorders. *Pharmaceuticals* **2024 (a)**, 17, 62.

8. Burloiu, A. M.; Mihai, D. P.; Manda, G.; Lupuliasa, D.; Neagoe, I. V.; Socoteanu, R. P.; Surcel, M.; Anghelache, L. I.; Olariu, L.; Gîrd, C. E.; Boscencu, R. In Silico and In Vitro Studies on an Asymmetrical Porphyrin Derivative with Therapeutic Potential in Skin Disorders. *Pharmaceuticals* **2024 (b)**, 17, 688.

9. Chavan, S.; Nicholls, I.A.; Karlsson, B.C.G.; Rosengren, A.M.; Ballabio, D.; Consonni, V.; Todeschini, R. Towards global QSAR model building for acute toxicity: Munro database case study. *Int. J. Mol. Sci*. **2014**, 15, 18162–18174.

10. Dobre, M.; Boscencu, R.; Neagoe, I.V.; Surcel, M.; Milanesi, E.; Manda, G. *Pharmaceutics* **2021**,13,1032.

11. Dodds, A.; Chia, S.; Shumack, S. *Dermatol Ther (Heidelb).* **2014**, 4, 11-31.

12. Esteva, A.; Kuprel, B.; Novoa, R.A.; Ko, J.; Swetter, S.M.; Blau, H.M.; Thrun, S. Dermatologist-level classification of skin cancer with deep neural networks. *Nature*. **2017**, 542, 7639.

13. Gouterman, M. Optical Spectra and Electronic Structure of Porphyrins and Related Rings, In The Porphyrins, Dolphin D., Ed. Academic Press: New York, NY, USA, 1978, Volume 3, 11–87.

14. Gouterman, M.; Wagniere, G. H.; Snyder, L. C. Spectra of porphyrins: Part II. Four orbital model. J. Mol. Spectrosc., 1963, 11, 108–127.

15. Kim, T.E; Chang, J.E. Recent Studies in Photodynamic Therapy for Cancer Treatment: From Basic Research to Clinical Trials. *Pharmaceutics. 2023*, 15, 2257.

16. Lomize, A.L.; Hage, J.M.; Schnitzer, K.; Golobokov, K.; LaFaive, M.B.; Forsyth, A.C.; Pogozheva, I.D. PerMM: A Web Tool and Database for Analysis of Passive Membrane Permeability and Translocation Pathways of Bioactive Molecules. *J. Chem. Inf. Model.* **2019**, 59, 3094–3099.

17. Luo, O.D.; Bose, R.; Bawazir, M.A.; Thuraisingam, T.; Ghazawi, F.M. A Review of the Dermatologic Clinical Applications of Topical Photodynamic Therapy. *J Cutan. Med. Surg*. **2024**, 28, 1-18.

18. Pandey, R.K.; Zheng, G. Porphyrins as photosensitizers in photodynamic therapy. In *The Porphyrin Handbook*; Kadish, K.M., Guilard, R., Smith, K.M., Eds.; Academic Press: New York, NY, USA, 2000; Volume 6, pp. 157–230.

19. Pires, D.E.V.; Blundell, T.L.; Ascher, D.B. pkCSM: Predicting small-molecule pharmacokinetic and toxicity properties using graph-based signatures. *Journal of Medicinal Chemistry* **2015**, 58, 4066–4072.

20. Plekhova, N.; Shevchenko, O.; Korshunova, O.; Stepanyugina, A.; Tananaev, I.; Apanasevich, V. Development of Novel Tetrapyrrole Structure Photosensitizers for Cancer Photodynamic Therapy. *Bioengineering* **2022**, *9*, 82.

21. Sarbadhikary, P.; George, B.P.; Abrahamse, H. Recent Advances in Photosensitizers as Multifunctional Theranostic Agents for Imaging-Guided Photodynamic Therapy of Cancer., *Theranostics* **2021**, 11, 9054-9088.

22. Simpson, M.C.; Novikova, I.N. Porphyrins: Electronic structure and ultraviolet/visible absorption spectroscopy. In *Fundamentals of Porphyrin Chemistry: A 21st Century Approach*; Brothers, P.J., Senge, O.M., Eds.; John Wiley & Sons Ltd.: New Jersey, NJ, USA, 2022; Volume 1, pp. 505–586.

23. Yang, H.; Lou, C.; Sun, L.; Li, J.; Cai, Y.; Wang, Z.; Tang, Y. AdmetSAR 2.0: Web-service for prediction and optimization of chemical ADMET properties. *Bioinformatics*, **2019**, 35, 1067–1069.

24. Yang, J.; Wang, S. Polysaccharide-Based Multifunctional Hydrogel Bio-Adhesives for Wound Healing: A Review. *Gels* **2023**, *9*, 138.

25. Yano, S.; Hirohara, S.; Obata, M.; Hagiya, Y.; Ogura, S.I.; Ikeda, A.; Kataoka, H.; Tanaka, M.; Joh, T. Current states and future views in photodynamic therapy, *Journal of Photochemistry and Photobiology C*: Photochemistry Reviews, **2011**, 12, 46– 67.

26. Zink, A. Trends in the treatment and prevention of keratinocyte carcinoma (non-melanoma skin cancer). *Curr Opin Pharmacol*. **2019**, 46, 19-23.

LIST OF PUBLISHED SCIENTIFIC PAPERS

Papers published in ISI journals

In silico and in vitro studies on an asymmetrical porphyrin derivative with therapeutic potential in skin disorders. **Burloiu, A. M.,** Mihai, D. P., Manda, G., Lupuliasa, D., Neagoe, I. V., Socoteanu, R. P., Surcel, M., Anghelache, L. I., Olariu, L., Gîrd, C. E., Boscencu, R. Pharmaceuticals, 17(6), 688, 2024 (F.I.=4.3, Q1), https://doi.org/10.3390/ph17060688.

Assessment of some unsymmetrical porphyrins as promising molecules for photodynamic therapy of cutaneous disorders. **Burloiu, A. M.,** Manda, G., Lupuliasa, D., Socoteanu, R. P., Mihai, D. P., Neagoe, I. V., Anghelache, L. I., Surcel, M., Anastasescu, M., Olariu, L., Gîrd, C. E., Barbuceanu, S. F., Ferreira, L. F. V., Boscencu, R. Pharmaceuticals, 17(1), 62, 2024 (F.I.=4.3, Q1), https://doi.org/10.3390/ph17010062.

Porphyrin photosensitizers into polysaccharide based biopolymer hydrogels for topical Photodynamic Therapy: Physicochemical and pharmacotechnical assessments. **Burloiu, A. M.**, Ozon, E. A., Musuc A. M., Anastasescu M., Socoteanu R. P., Atkinson, I., Culita D., Anuta, V., Popescu, I. A., Lupuliasa, D., Mihai, D. P., Gîrd, C. E., Boscencu, R. Gels, 2024 *10*, 499. (F.I.=5, Q1), https://doi.org/10.3390/gels10080499.

Patent

Porphyrinic compound with fluorescent marker potential in dermato-oncology, **Burloiu Andreea Mihaela,** Manda Gina, Boscencu Rica, Neagoe Ionela Victoria, Lupuliasa Dumitru, Surcel Mihaela, Olariu Laura, Mihai Dragos Paul. Patent application no. 202200775, published in RO-BOPI 5/30.05.2023.

Other ISI indexed papers

Porphyrin macrocycles: general properties and theranostic potential. Boscencu, R.; Radulea, N.; Manda, G.; Machado, I. F.; Socoteanu, R. P.; Lupuliasa, D.; **Burloiu, A.M.***; Mihai, D. P.; Ferreira Vieira, L. F. Molecules, 28(3), 11492023, 2023 (F.I.=4.2).

Interaction of some asymmetrical porphyrins with U937 cell membranes-in vitro and in silico studies. Mihai, D. P.; Boscencu, R.; Manda, G.; **Burloiu, A. M.***; Vasiliu, G.; Neagoe, I. V.; Socoteanu, R. P.; Lupuliasa, D. Molecules, 28(4), 1640, 2023 (F.I.=4.2).

Preliminary in vitro evaluation of some porphyrins using human breast tumor cells. Boscencu, R.; Manda, G.; Vasiliu, G.; Socoteanu, R. P.; Lupuliasa, D.; **Burloiu, A. M.**; Neagoe, I. V.; Olariu, L. Letters in Drug Design & Discovery, 20(8), 1040, 2023 (F.I.=1).